PCCP

Accepted Manuscript

ROYAL SOCIETY OF CHEMISTRY

www.rsc.org/pccp

Physical Chemistry Chemical Physics RSCPublishing

ARTICLE

Study of the chemical reactivity with relation to the experimental parameters of efficiency in coumarin derivatives for dye sensitized solar cells using DFT

Cite this: DOI: 10.1039/x0xx00000x

Received 00th January 2015,

Accepted 00th January 2015

DOI: 10.1039/x0xx00000x

www.rsc.org/

Rody Soto-Rojo[a,b], Jesus Baldenebro-López[b] and Daniel Glossman-Mitnik[a]

A group of dyes derived from coumarin was studied, which consisted of nine molecules with a very similar manufacturing process of the dye sensitized solar cells (DSSC). Optimized geometries, the energy levels of the highest occupied molecular orbital and the lowest unoccupied molecular orbital, and ultraviolet-visible spectra were obtained using theoretical calculations, and they were also compared with experimental conversion efficiencies of the DSSC. The representation of an excited state in terms of the natural transition orbitals (NTOs) was performed. Chemical reactivity parameters were calculated and correlated with the experimental data linked to the efficiency of the DSSC. A new proposal was obtained to design new molecular systems and to predict their potential use as a dye in DSSC.

1. Introduction

Dye sensitized solar cells (DSSC) promise to convert solar light to electricity more cheaply than silicon cells[1, 2] and with greater energy conversion efficiencies (η)[3-6]; however, so far the DSSC has only achieved efficiencies of 15% by perovskite sensitized solar cells[7], 12% by ruthenium based complexes dyes[8]. Metal free organic dyes have showed an outstanding advance in few years regarding to the conversion efficiency, such as: coumarins derivatives dyes up to 8%[9, 10], triphenylamine based up to 10%[5] using the I^-/I_3^- electrolyte. Recently, organic dyes have achieved higher conversion efficiencies up to 12.5% with carbazole[11] and indenoperylene[12] electron-donator based dyes and up to 12.8% with a triphenylamine based dye[13]. These latter using the cobalt complexes based electrolyte. Metal free organic dyes are the most advantageous because of its easy design and synthesis, and low cost[14, 15]; further, it demonstrates more possibilities for improving the efficiency. Hence the study and the understanding of the performance of metal free organic dyes are very important, and a useful and fast methodology for efficiency prediction is important as well. In this way, theoretical studies can effectively support the experimental research. In this sense, several organic dyes have been studied theoretically and experimentally, such as those based in triphenylamine[16-19] and coumarins[20-26]. Hara et al.[14, 27-30] have developed coumarin dyes that have been utilized as photosensitizers in dye sensitized solar cells that have reached high conversion efficiencies up to 8% [14]. On the other hand, the conversion efficiency depends on the used dye[31, 32] in the DSSC. Several researchers[25, 33-37] have carried out theoretical studies regarding NKX coumarin derivatives and have attempted to understand the relation between the molecular properties and the energy conversion efficiency of the DSSC. Some propose the necessity of using dye-TiO_2 complexes for correctly predicting the mechanism in the DSSC such as charge transfer or recombination; nevertheless, the relation of chemical reactivity of the dye with experimental data has not been studied for this group of molecules. Hence, a group of coumarin molecules was chosen for this study. This group was formed by different dyes evaluated in solar cells that were built and studied with a very similar construction process. The molecules for this study (C343, NKX-2398, NKX-2388, NKX-2311, NKX-2586, NKX-2753, NKX-2593, NKX-2807, and NKX-2883) are shown in Figure 1. The aim of this study was to calculate theoretical molecular properties and the chemical reactivity in order to compare and correlate with experimental data, such as short-circuit current density (J_{SC}), open-circuit voltage (V_{OC}), and energy conversion efficiency (η). Our goal was to obtain a methodology for the efficient selection of Donor-π linker-Acceptor (D-π-A) type dyes.

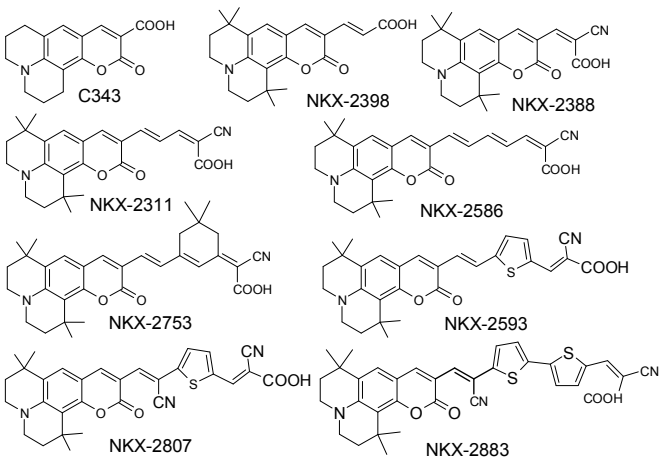

Fig. 1 Structure of Coumarin derivative dyes.

2. Calculation Details

Theoretical study has been carried out using density functional theory (DFT) by the B3LYP[38] and PBE0[39] hybrid GGA functionals and the M06[40] hybrid meta-GGA functional combined with two basis sets: the 6-31G(d)[41, 42] proposed by Pople and MIDIY[43] developed by the Truhlar group at the University of Minnesota. Furthermore, the CAM-B3LYP[44] range-separated hybrid functional was used with 6-31G(d). Ground state geometry optimization, energy levels of the highest occupied molecular orbital (HOMO) and the lowest unoccupied molecular orbital (LUMO), and the chemical reactivity parameters were obtained. The chemical reactivity parameters were obtained by energy calculations (ionic and neutral state)[45, 46]. Ultraviolet-visible (UV-Vis) spectra were calculated in ethanol using the Time-Dependent DFT (TD-DFT) with the non-equilibrium protocol[47, 48] and were processed by Swizard program[49, 50] using the Gaussian model to read the oscillator strength (f) and the orbitals involved in the electron transitions. A possible improvement to get a deeper understanding of the nature of the electronic transitions leans on the representation of an excited state in terms of the natural transition orbitals (NTOs)[51]. By performing a singular value decomposition of the transition density matrix, one may express the excited state as a transition from occupied to virtual NTO. The equations were solved for 20 excited states, and the solvent effect was considered by the integral equation formalism polarizable continuum model (IEF-PCM)[52], an implicit method. All levels calculated were similar with exception of CAM-B3LYP, but PBE/MIDIY, PBE/6-31G(d) and M06/6-31G(d) presented the most accurate results. The other theoretical models (M06/MIDIY, B3LYP/6-31G[d], B3LYP/MIDIY and CAM-B3LYP/6-31G[d]) are available in the electronic supplementary material. Values of maximum wavelength (λ_{max}) and its electron transition were compared for different experimental efficiencies as well as the difference in energy between the dye LUMO and the TiO_2 semiconductor conduction band. Further, molecular properties and the chemical reactivity were correlated with experimental data, such as short circuit current density (J_{SC}), open circuit voltage (V_{OC}), and the light conversion efficiency. Pearson correlation and P value were calculated to choose the best correlation. All calculations were carried out with the Gaussian 09 Revision D.01[53].

3. Results and Discussions

The maximum absorption wavelength (nm), the oscillator strengths, the electron transitions, and the HOMO and LUMO were studied and analyzed to choose the best molecule to be used in DSSC. Furthermore, the Pearson correlation was calculated to obtain relations between the chemical reactivity and the experimental results of conversion efficiency. The latter were reported for the group of Hara[28-30] and are shown in Table 1. All levels of theory used describe similarly and the calculated molecular properties exhibit the same trend, with exception of CAM-B3LYP/6-31G(d). Therefore, only the most approximate level to experimental maximum wavelengths is shown here, M06/6-31G(d). Other theoretical models can be found in the electronic supplementary information (ESI).

Table 1 Experimental data of the conversion efficiency and maximum wavelength (λ_{max}) in ethanol of coumarin dyes.

Molecule	λ_{max} (nm)	J_{SC} (mA/cm^2)	V_{OC} (V)	FF	η (%)
C343	442	4.1	0.41	0.56	0.9
NKX-2398	451	11.1	0.51	0.60	3.4
NKX-2388	493	12.9	0.50	0.64	4.1
NKX-2311	504	15.2	0.55	0.62	5.2
NKX-2586	506	15.1	0.47	0.50	3.5
NKX-2753	492	16.9	0.54	0.63	5.7
NKX-2593	510	16.71	0.52	0.67	5.8
NKX-2807	566	14.32	0.51	0.73	5.3
NKX-2883	552	17.46	0.52	0.69	6.3

Experimental data reported for Hara et al.[22-24]

3.1 Ultraviolet-visible spectra.

The values of theoretical and experimental maximum wavelengths are shown in the table 2 for its comparison. Considering all the systems studied, shorter molecules (without π bridge) and the longer molecules (with larger π bridge), M06 functional presents the best alternative according to the levels of calculation proposed here. If the main interesting is to obtain the UV-Vis spectra with a good accurate, it can be resolved using functionals with minor and major Hartree Fock (HF) exchange according to Dev *et al.*[54]. A good option could be M06-L and M06-2X for shorter and longer molecules, respectively. In this case, we need to use only a functional for to compare suitably the absorption theoretical data among the different molecules.

Table 2 Comparison between the theoretical and experimental maximum absorption wavelengths (λ_{max}) .

Molecule	Theoretical λ_{max}	Experimental λ_{max}	Difference
C343	376	442	66
NKX-2398	400	451	51
NKX-2388	424	493	69
NKX-2311	494	504	10
NKX-2586	519	506	13
NKX-2753	525	492	33
NKX-2593	576	510	66
NKX-2807	560	566	6
NKX-2883	651	552	99

All units are in nm.

The theoretical ultraviolet-visible absorption spectra of the nine coumarin derivative dyes obtained with the M06/6-31G(d) level of theory are shown in Figure 2. It was observed that more redshifted maximum wavelength corresponded to better experimental conversion efficiency, excluding the NKX-2586 and NKX-2807. The above is due to the value of λ_{max}, which is related to the HOMO-LUMO energy gap. Generally, when a dye absorbs closer to red where the energy of the light is minor, the LUMO energy level is more negative; therefore, it is closer to the TiO_2 conduction band[55]. On the other hand, it was observed that the molecules with a λ_{max} above 400 nm had a similar experimental efficiency; this region coincides with the area of greatest solar radiation[56-58]. In this study, it is important to emphasize that all signals of maximum wavelengths (λ_{max}) correspond to HOMO to LUMO (H→L) transitions, which are shown in Table 3. Further there were others signals blueshifted with transitions involving different orbitals such as HOMO-1→LUMO and HOMO→LUMO+1 that also contributed in the light harvesting. Some authors consider the value of f (using the LHE: Light Harvesting Efficiency) to be directly proportional with the J_{SC} in order to predict the molecule with the best efficiency[19, 37, 59, 60]; however, in molecules having several signals of absorption involved in the harvesting and the energy transfer, it is very difficult to select the best molecule with this criteria.

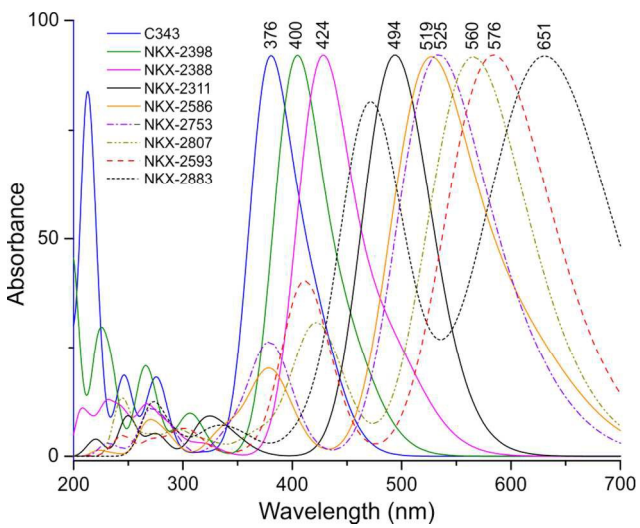

Fig. 2 Theoretical UV-Vis spectra of coumarin derivative dyes using M06/6-31G(d).

3.2 Energy levels of the molecular orbitals.

In relation to the absorption spectra analysis and the electron transitions between the orbitals, it is important to observe the HOMO, HOMO-1, LUMO, and LUMO+1 energy levels that are shown in Figure 3; these are the orbitals involved in such electron transitions. It is known that in a dye the position of the LUMO level must be above the conduction band (CB) of the TiO_2 semiconductor (-4.0 eV)[61], and the HOMO level should be below the redox potential of the I^-/I_3^- electrolyte (-4.8 eV)[61] to allow for charge injection from the dye to TiO_2 as well as the regeneration of the dye that receives electrons from the electrolyte. It can be observed that all molecules are appropriate candidates as photosensitizers. Furthermore, a general tendency was noted: a lower LUMO energy level resulted generally in higher conversion efficiency, excluding NKX-2586 and NKX-2807. If NKX-2311 and NKX-2753 are compared, the former has a more negative LUMO level and a lower efficiency than the latter, but NKX-2753 has a minor band gap, and may require the HOMO level closer to the redox potential than the NKX-2311, allowing a better efficiency. On the other hand, the DSSC with NKX-2753 received a treatment of $TiCl_4$ in the TiO_2 that creates a slightly higher efficiency. NKX-2807 and NKX-2883 also were measured in DSSCs that received the aforementioned treatment. Despite that NKX-2807 has a lower LUMO level than NKX-2883, it has a lower efficiency. However, it can be observed that both LUMO levels were very similar, and NKX-2883 has the HOMO level closer to the redox potential; therefore, there is a lower band gap. Also, it presented a second transition HOMO→LUMO+1 and HOMO-1→LUMO with a smaller band gap than NKX-2807, which also contributes to the light harvesting.

Table 3 Absorption wavelengths, oscillator strength (f), and the orbitals involved in the transitions of coumarins using M06/6-31G(d).

Molecule	λ_{max} (nm)	f	Transitions H=HOMO L=LUMO (%)
C343	376	0.6484	H→L(97)
	275	0.0995	H→L+1(84)
	219	0.1070	H→L+3(74)
	211	0.4694	H-1→L+1(75)
NKX-2398	400	0.9909	H→L(99)
	306	0.0867	H→L+1(83)
	264	0.1828	H-2→L(55) H→L+2(31)
	223	0.1551	H-2→L+1(84)
NKX-2388	424	1.1066	H→L(99)
	265	0.0991	H→L+2(72)
	245	0.0792	H-1→L+1(88)
	229	0.0511	H-2→L+1(57) H-7→L(24)
NKX-2311	494	1.7517	H→L(99)
	321	0.1478	H-1→L(63)
	276	0.0961	H→L+2(80)
	252	0.0817	H-2→L+1(79)
NKX-2586	519	1.8326	H→L(100)
	381	0.3357	H→L+1(49) H-1→L(44)
	336	0.1348	H-1→L(52) H→L+1(41)
	269	0.0703	H-3→L(36) H-1→L+1(35)
NKX-2753	525	1.5791	H→L(100)
	380	0.4221	H→L+1(54) H-1→L(43)
	286	0.0572	H→L+2(51) H-2→L+1(21)
	268	0.1028	H-2→L+1(63) H→L+2(28)
NKX-2593	576	1.4079	H→L(100)
	412	0.7190	H-1→L(52) H→L+1(47)
	314	0.0437	H→L+2(88)
	245	0.0441	H→L+6(46) H-1→L+2(25)
NKX-2807	560	1.3953	H→L(100)
	423	0.5691	H→L+1(74) H-1→L(24)
	367	0.0854	H-1→L(60) H→L+1(19) H-2→L(18)
	244	0.1027	H-4→L+1(51) H-2→L+2(29)
NKX-2883	651	0.9998	H→L(99)
	476	1.2480	H→L+1(50) H-1→L(48)
	325	0.0515	H-3→L(42) H-1→L+1(27)
	273	0.0855	H-1→L+2(28) H-5→L(21)

Mapping of the HOMO and LUMO orbitals is important for observing the charge separation; hence, it was obtained and analyzed in the Figure 4. It can be observed that all molecules present a charge distribution like a photosensitizer[62], namely, the HOMO density was mostly concentrated in the coumarin donator region, while the LUMO density was in the cyanoacrylic acid acceptor region where the TiO_2 semiconductor is attached. Furthermore, as the π bridge was increased with vinylene chains, thiophenes or phenyl, a better charge separation was obtained, although there is still overlap of the orbitals. Moreover, the NKX-2311 and NKX-2586 molecules were compared, and despite that both have qualitatively the same HOMO and LUMO charge distribution, NKX-2311 presented a higher efficiency. Besides, NKX-2586 was more redshifted and nearer to the TiO2 conduction band than NKX-2311; therefore, theoretically NKX-2586 was estimated as the best among them, however, Hara[28] and co-workers reported that NKX-2586 had a low efficiency due to aggregation on the TiO2, according to experimental results. Due to the above, NKX-2586 was considered like an exception in our methodology of study.

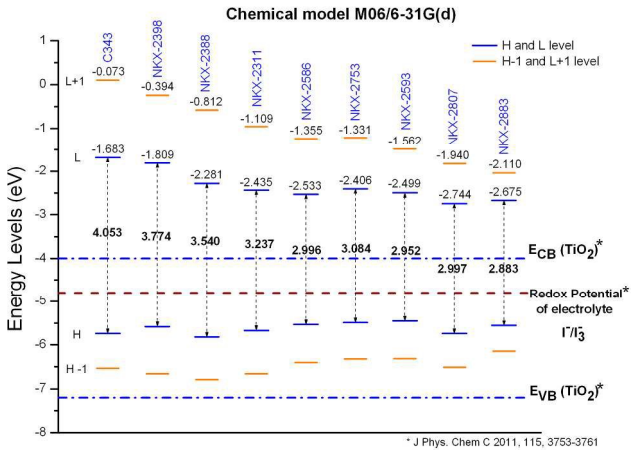

Fig. 3 Orbitals energy levels of coumarins derivative dyes at M06/6-31G(d) level of calculation.

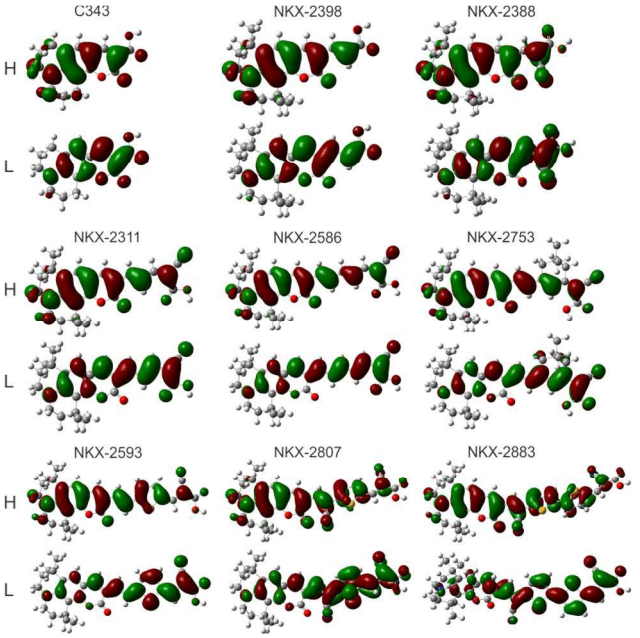

Fig. 4 HOMO and LUMO molecular orbitals at the M06/6-31G(d) level of calculation.

Moreover, in the paper of NKX-2807[30], Hara and co-workers expected a higher efficiency for this dye, for example, compared with NKX-2593, but this was not the case because NKX-2807 had a lower IPCE (Incident photon-to-electron conversion efficiency) that was related with the driving force of the electron injection (the difference between LUMO and TiO_2 conduction band edge). These researchers expected that a molecule with higher electron-withdrawing ability had higher conversion efficiency (η) and hypothesized that "the electrons first move from the donor part to the –CN group linked to the π-conjugation bridge, upon excitation, and then move to the ending acceptor part (i.e., cyanoacrylic acid)". In this case, the

problem was that the CN group attached to NKX-2593 (in the π bridge before thiophene) to obtain the NKX-2807 increased the electron-withdrawing ability, but it was concentrated partly in this group and partly in the cyanoacrylic acid as is shown in Figure 4. Hence the CN group perhaps interrupted the charge transfer instead of serving as a springboard. This leads to the idea that a dye need to have mainly the LUMO orbital in the anchor group instead of the π-bridge as the case of NKX-2807 that has a structure of D-A-π-A; note that it was seen that adding the CN did not lead to a good result. NKX-2883 also has a D-A-π-A structure; however, the –CN group is more separated from the cyanoacrylic acid. Therefore, the LUMO was not as concentrated in this group.

The nature of the first excited state can be determined by analyzing the corresponding NTOs (Figure 5). As expected, the results for the transition of the most intense band are consistent with the HOMO and LUMO orbitals of the Figure 4. The excitation promoting an electron from an orbital that is dominantly on the coumarin donor region to one that is localized on the anchoring group (cyanoacrylic acid); the transition can be entirely described as electron removal from the occupied NTO ("hole" density) and electron accumulation into the virtual NTO ("particle" density). Orbitals separation is more evident when the π bridge increases in size.

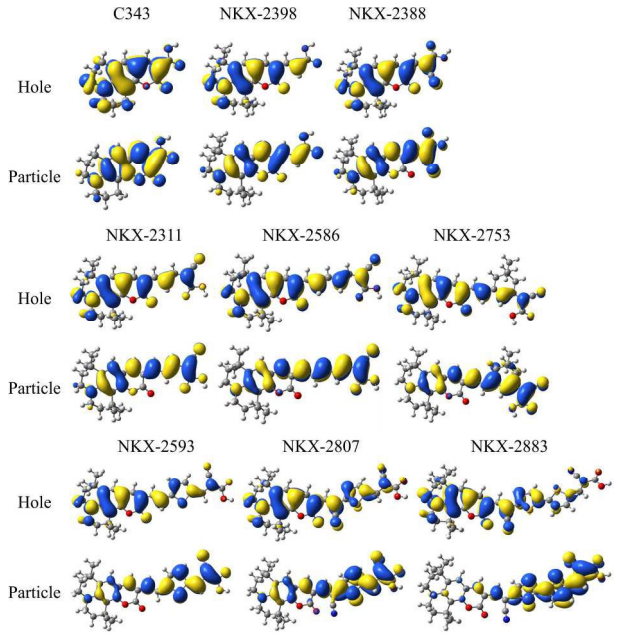

Fig. 5 Dominant natural transition orbital pair for the first excited singlet state of coumarin molecules with M06/6-31G(d) level of calculation.

Electron Density Difference Maps (EDDMs) for the first excited singlet state with the M06/6-31G(d) level of theory was included in ESI (Figure S3). The EDDMs show the changes in electron density for a given excitation, where the electron density loss in the excitation is represented in cyan, and the purple color indicates the electron density gain.

3.3 Chemical reactivity and correlation study.

Using the molecular energies for the ionic and neutral species, the following chemical reactivity parameters were calculated (in eV): electron affinity (A), ionization potential (I), chemical hardness (h), electrophilicity index (ω), electrodonating power (ω-), and electroaccepting power (ω+). The values are shown in the Table 4.

Table 4 Chemical reactivity of coumarin derivatives dyes at M06/6-31G(d).

MOLECULE	A	I	h	ω	ω-	ω+
C343	0.32	7.03	3.36	2.02	4.27	0.60
NKX-2398	0.60	6.74	3.07	2.19	4.41	0.74
NKX-2388	1.11	6.94	2.91	2.78	5.16	1.13
NKX-2311	1.34	6.71	2.69	3.01	5.36	1.34
NKX-2586	1.51	6.53	2.51	3.21	5.54	1.52
NKX-2753	1.41	6.45	2.52	3.06	5.35	1.41
NKX-2593	1.48	6.41	2.46	3.15	5.43	1.49
NKX-2807	1.77	6.68	2.46	3.64	6.06	1.83
NKX-2883	1.76	6.44	2.34	3.58	5.92	1.83

A=electron affinity, I=ionization potential, h=chemical hardness, ω=electrophilicity index, ω-=electrodonating power, and ω+=electroaccepting power. All units are in eV.

Mainly, chemical hardness is an important datum that represents the resistance to intramolecular charge transfer[45, 63]; hence, a lower chemical hardness is desired. Figure 6 shows a graph of chemical hardness (Table 4) and experimental efficiency (Table 1) of each coumarin molecule. It can be observed that the conversion efficiency increases, while the chemical hardness decreases. Exceptions again are NKX-2586 and NKX-2807, as explained above.

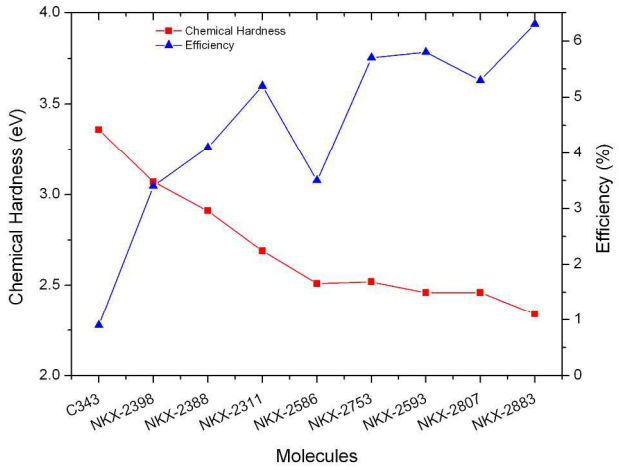

Fig. 6 Chemical hardness and experimental efficiency of coumarin molecules.

On the basis of the above results, we thought of performing calculations of Pearson correlation coefficients between the chemical reactivity and experimental efficiency parameters shown in Table 5, excluding the exception molecules NKX-2586 and NKX-2807. Taking into account that the Pearson correlation coefficient is a measure of the linear relation among two random variables quantitative, and if P-value <

0.05 is obtained, it can be assumed that there really is a strength of association between the two variables[64]. We used the method above to find a relation between the theoretical molecular properties and the experimental results that could predict new D-π-A molecular systems. Furthermore, the strengh oscillator (f) and the driving force of the electron injection (inject) were correlated. Electron affinity and ionization potential were not discussed since these are used for obtaining the rest of the chemical reactivity and can be redundant. A important aim was to consider a group of D-π-A dyes used in DSSCs with the same conditions of manufacture and measurement. The aim is obtaining a reliable comparison among them, althougth the number of molecules is small, therefore the results should be taken into account with caution. Despite only seven data were correlated, good results were obtained, namely, the chemical reactivity and the driving force of electron injection have an effect on the parameters of efficiency. For example, chemical hardness has an excellent correlation with η (-0.977), Jsc (-0.960), and driving force of electron injection (0.955); furthermore, it had P-values near zero: 0.001, 0.001 and 0.000, respectively. The effect of the theoretical results in each experimental datum can be analyzed. For example, the Jsc was inversely proportional correlated with chemical harness (-0.960, P=0.001) and inject (-0.923, P=0.003); this means that the best Jsc is obtained when the chemical hardness and the inject are smaller. The smaller inject corresponds to a LUMO energy level that is nearer to the TiO_2 conduction band. Besides, Jsc presented an excellent positive correlation with electrophilicity (0.912, P=0.004) and electroaccepting power (0.911, P=0.004), meaning that the higher energetic stability and electron-withdrawing ability result in a better Jsc and consequently in a better conversion efficiency (η). NKX-2807 has the same electroaccepting power as NKX-2883, but it should be concentrated in the anchor group. The electrodonating power presented a positive correlation with Jsc (0.897, P=0.006). This means that a higher electrodonating power represents a lower electrondonating ability[38], namely, the molecule with the lowest electrodonating capacity has the better efficiency in this study. Otherwise, the Voc had similar Pearson correlations to Jsc, but with poorer values. An exception was the oscillator strength where Voc and Jsc presented 0.717 (P=0.017) and 0.845 (P=0.070), respectively. Although the oscillator strength was obtained from the maximum wavelength and other absorptions were not considered, it presented a seemly correlation with the experimental data, which show an effect on them (e.g., the efficiency; Pearson correlation=0.693, P=0.084).

Table 5 Pearson correlation and P-Value of coumarin derivatives between the theoretical molecular properties and chemical reactivity, the oscillator strength, and driving force of the electron injection (inject).

PARAMETER	Jsc	Voc	η	inject
Chemical Hardness	-0.960 0.001	-0.774 0.041	-0.977 0	0.955 0.001
Electrophilicity	0.912 0.004	0.700 0.080	0.937 0.002	-0.990 0
Electrodonating power	0.897 0.006	0.689 0.087	0.921 0.003	-0.993 0
Electroaccepting power	0.911 0.004	0.691 0.086	0.938 0.002	-0.982 0
Oscillator strength	0.717 0.070	0.845 0.017	0.693 0.084	-0.622 0.136
inject	-0.923 0.003	-0.738 0.058	-0.942 0.002	

Cell contents: Pearson correlation and P-Value.

The η is mainly affected with the same tendency as Jsc. Hence, the η will be better when the Jsc is higher, but it also has a higher Voc. Finally, the driving force of electron injection (inject) resulted smaller with the lowest chemical hardness, and higher electrophilicity, electrodonating power, and electroacepting power, and in general with a higher oscillator strength. A first selection criteria could be addressed to molecules with a lower chemical hardness and driving force of electron injection and also a higher electrophilicity and electroaccepting power. It is important to note that there should be an equilibrium between electroaccepting power and electrodonating power. For example, Table 4 shows that NKX-2807 and NKX-2883 have the same electroaccepting power, but NKX-2807 has a higher electrodonating power, namely, both have the same electron-withdrawing ability, but NKX-2807 has less electrodonating ability than NKX-2883. Consequently, this sensitizer has the highest conversion efficiency (η). The Pearson correlation coefficients reported here were consistent with those obtained by the other chemical models included in the electronic supplementary material (ESI).

3. Conclusions

The methodology employed in this study that was used to select the molecule with the best conversion efficiency (η) was in accordance with the experimental data, i.e., both showed that NKX-2883 was the best dye of this group. Also, the driving force of electron injection is a useful criteria to choose the best dye; however, the chemical reactivity parameters, mainly chemical hardness, electrophilicity, electrodonating power, and electroaccepting power, allow a deeper study for predicting the dye with the highest efficiency, and it can be an auxiliary supporting and previous to calculations of the dye-TiO2 complex. According to the above, if a big group of molecules is studied, it can be reduced to a little group to be synthesized and used in DSSC, by simply performing calculations of geometry optimization and subsequently searching the smaller chemical hardness and inject as well as looking for

higher electrophilicity and electroaccepting power. In this sense, it was observed that the π bridge had an important effect on the properties of the dyes. When the conjugation of the π bridge is augmented, the dye presents a lower chemical hardness and the LUMO energy is closer to the TiO_2 conduction band. Consequently, there is higher electrophilicity and electroaccepting power. The above parameters have a good correlation with the experimental efficiency parameters. Also, f was positively affected by the π bridge conjugation. Therefore, these molecular systems can be studied in the future.

Acknowledgements

This work was supported by Consejo Nacional de Ciencia y Tecnología (CONACYT), Centro de Investigación en Materiales Avanzados, S.C. (CIMAV), and Universidad Autónoma de Sinaloa (UAS). R.S.R. gratefully acknowledge a fellowship from CONACYT. D.G.M is a researcher of CIMAV and CONACYT. J.B.L is professor and researcher at the UAS.

Notes and references

[a] Laboratorio Virtual NANOCOSMOS - Departamento de Medio Ambiente y Energía - Centro de Investigación en Materiales Avanzados - Miguel de Cervantes 120, Complejo Industrial Chihuahua, Chihuahua, Chih. 31136 - México.

[b] Facultad de Ingeniería Mochis - Universidad Autónoma de Sinaloa - Prol. Ángel Flores y Fuente de Poseidón, S.N, C.P. 81223 Los Mochis, Sinaloa, México.

† Electronic Supplementary Information (ESI) available: The theoretical results with the B3LYP and PBE0 hybrid GGA functionals, the M06 hybrid meta-GGA functional and the CAM-B3LYP44 range-separated hybrid functional were included. Two basis set were used: 6-31G(d) and MIDIY. See DOI: 10.1039/b000000x/

1. B. O'Regan and M. Gratzel, *Nature*, 1991, **353**, 737-740.
2. M. Grätzel, *Journal of Photochemistry and Photobiology C: Photochemistry Reviews*, 2003, **4**, 145-153.
3. M. K. Nazeeruddin, F. De Angelis, S. Fantacci, A. Selloni, G. Viscardi, P. Liska, S. Ito, B. Takeru and M. Grätzel, *Journal of the American Chemical Society*, 2005, **127**, 16835-16847.
4. A. Hagfeldt, G. Boschloo, L. Sun, L. Kloo and H. Pettersson, *Chemical Reviews*, 2010, **110**, 6595-6663.
5. W. Zeng, Y. Cao, Y. Bai, Y. Wang, Y. Shi, M. Zhang, F. Wang, C. Pan and P. Wang, *Chemistry of Materials*, 2010, **22**, 1915-1925.
6. A. Yella, H.-W. Lee, H. N. Tsao, C. Yi, A. K. Chandiran, M. K. Nazeeruddin, E. W.-G. Diau, C.-Y. Yeh, S. M. Zakeeruddin and M. Grätzel, *Science*, 2011, **334**, 629-634.
7. J. Burschka, N. Pellet, S.-J. Moon, R. Humphry-Baker, P. Gao, M. K. Nazeeruddin and M. Gratzel, *Nature*, 2013, **499**, 316-319.
8. H. Ozawa, Y. Okuyama and H. Arakawa, *ChemPhysChem*, 2014, **15**, 1201-1206.
9. K. Hara, Z.-S. Wang, T. Sato, A. Furube, R. Katoh, H. Sugihara, Y. Dan-oh, C. Kasada, A. Shinpo and S. Suga, *The Journal of Physical Chemistry B*, 2005, **109**, 15476-15482.
10. Z.-S. Wang, Y. Cui, Y. Dan-oh, C. Kasada, A. Shinpo and K. Hara, *The Journal of Physical Chemistry C*, 2007, **111**, 7224-7230.
11. K. Kakiage, Y. Aoyama, T. Yano, T. Otsuka, T. Kyomen, M. Unno and M. Hanaya, *Chemical Communications*, 2014, **50**, 6379-6381.
12. Z. Yao, M. Zhang, H. Wu, L. Yang, R. Li and P. Wang, *Journal of the American Chemical Society*, 2015, **137**, 3799-3802.
13. M. Zhang, Y. Wang, M. Xu, W. Ma, R. Li and P. Wang, *Energy & Environmental Science*, 2013, **6**, 2944-2949.
14. K. Hara, T. Sato, R. Katoh, A. Furube, T. Yoshihara, M. Murai, M. Kurashige, S. Ito, A. Shinpo, S. Suga and H. Arakawa, *Advanced Functional Materials*, 2005, **15**, 246-252.
15. D. P. Hagberg, T. Marinado, K. M. Karlsson, K. Nonomura, P. Qin, G. Boschloo, T. Brinck, A. Hagfeldt and L. Sun, *The Journal of Organic Chemistry*, 2007, **72**, 9550-9556.
16. S. Hwang, J. H. Lee, C. Park, H. Lee, C. Kim, C. Park, M.-H. Lee, W. Lee, J. Park, K. Kim, N.-G. Park and C. Kim, *Chemical Communications*, 2007, 4887-4889.
17. C.-R. Zhang, Z.-J. Liu, Y.-H. Chen, H.-S. Chen, Y.-Z. Wu, W. Feng and D.-B. Wang, *Current Applied Physics*, 2010, **10**, 77-83.
18. J. Liu, D. Zhou, F. Wang, F. Fabregat-Santiago, S. G. Miralles, X. Jing, J. Bisquert and P. Wang, *The Journal of Physical Chemistry C*, 2011, **115**, 14425-14430.
19. J. Zhang, Y.-H. Kan, H.-B. Li, Y. Geng, Y. Wu and Z.-M. Su, *Dyes and Pigments*, 2012, **95**, 313-321.
20. K. Hara, T. Sato, R. Katoh, A. Furube, Y. Ohga, A. Shinpo, S. Suga, K. Sayama, H. Sugihara and H. Arakawa, *The Journal of Physical Chemistry B*, 2002, **107**, 597-606.
21. K. Hara, Y. Dan-oh, C. Kasada, Y. Ohga, A. Shinpo, S. Suga, K. Sayama and H. Arakawa, *Langmuir*, 2004, **20**, 4205-4210.
22. K. D. Seo, H. M. Song, M. J. Lee, M. Pastore, C. Anselmi, F. De Angelis, M. K. Nazeeruddin, M. Gräetzel and H. K. Kim, *Dyes and Pigments*, 2011, **90**, 304-310.
23. K. D. Seo, I. T. Choi, Y. G. Park, S. Kang, J. Y. Lee and H. K. Kim, *Dyes and Pigments*, 2012, **94**, 469-474.

24. R. Sánchez-de-Armas, J. Oviedo, M. Á. San Miguel and J. F. Sanz, *The Journal of Physical Chemistry C*, 2011, **115**, 11293-11301.
25. R. Sanchez-de-Armas, M. A. San Miguel, J. Oviedo and J. F. Sanz, *Physical Chemistry Chemical Physics*, 2012, **14**, 225-233.
26. R. Sánchez-de-Armas, M. A. San-Miguel, J. Oviedo and J. F. Sanz, *The Journal of Chemical Physics*, 2012, **136**, -.
27. K. Hara, M. Kurashige, Y. Dan-oh, C. Kasada, A. Shinpo, S. Suga, K. Sayama and H. Arakawa, *New Journal of Chemistry*, 2003, **27**, 783-785.
28. K. Hara, Y. Tachibana, Y. Ohga, A. Shinpo, S. Suga, K. Sayama, H. Sugihara and H. Arakawa, *Solar Energy Materials and Solar Cells*, 2003, **77**, 89-103.
29. Z.-S. Wang, K. Hara, Y. Dan-oh, C. Kasada, A. Shinpo, S. Suga, H. Arakawa and H. Sugihara, *The Journal of Physical Chemistry B*, 2005, **109**, 3907-3914.
30. Z.-S. Wang, Y. Cui, Y. Dan-oh, C. Kasada, A. Shinpo and K. Hara, *The Journal of Physical Chemistry C*, 2008, **112**, 17011-17017.
31. K. Wongcharee, V. Meeyoo and S. Chavadej, *Solar Energy Materials and Solar Cells*, 2007, **91**, 566-571.
32. G. C. Vougioukalakis, A. I. Philippopoulos, T. Stergiopoulos and P. Falaras, *Coordination Chemistry Reviews*, 2011, **255**, 2602-2621.
33. X. Zhang, J.-J. Zhang and Y.-Y. Xia, *Journal of Photochemistry and Photobiology A: Chemistry*, 2008, **194**, 167-172.
34. S. Agrawal, P. Dev, N. J. English, K. R. Thampi and J. M. D. MacElroy, *Journal of Materials Chemistry*, 2011, **21**, 11101-11108.
35. E. Maggio, N. Martsinovich and A. Troisi, *The Journal of Physical Chemistry C*, 2012, **116**, 7638-7649.
36. C. Oprea, P. Panait, F. Cimpoesu, M. Ferbinteanu and M. Gîrţu, *Materials*, 2013, **6**, 2372-2392.
37. J. Wang, M. Li, D. Qi, W. Shen, R. He and S. H. Lin, *RSC Advances*, 2014, **4**, 53927-53938.
38. A. D. Becke, *The Journal of Chemical Physics*, 1993, **98**, 5648-5652.
39. C. Adamo and V. Barone, *The Journal of Chemical Physics*, 1999, **110**, 6158-6170.
40. Y. Zhao and D. Truhlar, *Theor Chem Acc*, 2008, **120**, 215-241.
41. M. M. Francl, W. J. Pietro, W. J. Hehre, J. S. Binkley, M. S. Gordon, D. J. DeFrees and J. A. Pople, *The Journal of Chemical Physics*, 1982, **77**, 3654-3665.
42. V. A. Rassolov, M. A. Ratner, J. A. Pople, P. C. Redfern and L. A. Curtiss, *Journal of Computational Chemistry*, 2001, **22**, 976-984.
43. B. J. Lynch and D. G. Truhlar, *Theor Chem Acc*, 2004, **111**, 335-344.
44. T. Yanai, D. P. Tew and N. C. Handy, *Chemical Physics Letters*, 2004, **393**, 51-57.
45. R. G. Parr and R. G. Pearson, *Journal of the American Chemical Society*, 1983, **105**, 7512-7516.
46. J. L. Gázquez, A. Cedillo and A. Vela, *The Journal of Physical Chemistry A*, 2007, **111**, 1966-1970.
47. M. Cossi and V. Barone, *The Journal of Chemical Physics*, 2001, **115**, 4708-4717.
48. R. Improta, V. Barone, G. Scalmani and M. J. Frisch, *The Journal of Chemical Physics*, 2006, **125**, -.
49. S. I. Gorelsky, University of Ottawa, Ottawa, Canada, 2013.
50. S. I. Gorelsky and A. B. P. Lever, *Journal of Organometallic Chemistry*, 2001, **635**, 187-196.
51. R. L. Martin, *The Journal of Chemical Physics*, 2003, **118**, 4775-4777.
52. E. Cancès, B. Mennucci and J. Tomasi, *The Journal of Chemical Physics*, 1997, **107**, 3032-3041.
53. T. G. Frisch MJ, Schlegel HB,, R. M. Scuseria GE, Cheeseman JR, Scalmani G, Barone V,, P. G. Mennucci B, Nakatsuji H, Caricato M, Li X,, I. A. F. Hratchian HP, Bloino J, Zheng G, Sonnenberg, H. M. JL, Ehara M, Toyota K, Fukuda R, Hasegawa J, Ishida, N. T. M, Honda Y, Kitao O, Nakai H, Vreven T,, P. J. Montgomery JA Jr, Ogliaro F, Bearpark M, Heyd JJ,, K. K. Brothers E, Staroverov VN, Kobayashi R, Normand J,, R. A. Raghavachari K, Burant JC, Iyengar SS, Tomasi J,, R. N. Cossi M, Millam NJ, Klene M, Knox JE, Cross JB,, A. C. Bakken V, Jaramillo J, Gomperts R, Stratmann RE,, A. A. Yazyev O, Cammi R, Pomelli C, Ochterski J W, Martin, M. K. RL, Zakrzewski VG, Voth GA, Salvador P,, D. S. Dannenberg JJ, Daniels AD, Farkas Ö, Foresman and O. J. JB, Cioslowski J, Fox DJ, Gaussian, Inc., Wallingford CT, 2009.
54. P. Dev, S. Agrawal and N. J. English, *The Journal of Chemical Physics*, 2012, **136**, 224301.
55. M. A. Green, *Solar Cells: Operating Principles, Technology, And System Applications*, Prentice-Hall, Englewood Cliffs, New Jersey, USA, 1982.
56. G. P. Smestad, *Optoelectronics of Solar Cells*, Society of Photo Optical, 2002.
57. P. Würfel and U. Würfel, *Physics of Solar Cells: From Basic Principles to Advanced Concepts*, Wiley, 2009.
58. A. McEvoy, L. Castaner and T. Markvart, *Solar Cells: Materials, Manufacture and Operation*, Elsevier Science, 2012.
59. J. Zhang, H.-B. Li, Y. Geng, S.-Z. Wen, R.-L. Zhong, Y. Wu, Q. Fu and Z.-M. Su, *Dyes and Pigments*, 2013, **99**, 127-135.
60. A. K. Biswas, S. Barik, A. Sen, A. Das and B. Ganguly, *The Journal of Physical Chemistry C*, 2014, **118**, 20763-20771.
61. X. Lu, S. Wei, C.-M. L. Wu, S. Li and W. Guo, *The Journal of Physical Chemistry C*, 2011, **115**, 3753-3761.

62. K. R. J. Thomas, N. Kapoor, C.-P. Lee and K.-C. Ho, *Chemistry – An Asian Journal*, 2012, **7**, 738-750.
63. J. Martínez, *Chemical Physics Letters*, 2009, **478**, 310-322.
64. D. C. LeBlanc, *Statistics: Concepts and Applications for Science*, Jones and Bartlett, 2004.